Comparisons of Two UCAV Wing Designs Including Low-Speed Experimental Verification

Dr. R. K. Nangia*, Ir. O.J. Boelens, Mr. Magnus Tormalm*****

*** Consulting Aeronautical Engineer, Nangia Aero Research Associates**
WestPoint, 78-Queens Road, Clifton, BRISTOL, BS8 1QU, UK.

****R&D Engineer, Applied Computational Fluid Dynamics**
Department of Flight Physics and Loads, Aerospace Vehicles Division
NLR, Amsterdam, Netherlands

*****Senior Scientist, Applied Computational Fluid Dynamics**
Aeronautics and Systems Integration
FOI, Stockholm, Sweden

Keywords: Aircraft Design, UCAV, CFD

ABSTRACT

The subject of UCAV design is an important current topic. Many countries have their own programmes. An International group is under the initiative of the NATO RTO-AVT-161 Task group (assessment of Stability and Control Prediction Methods for NATO Air and Sea Vehicles -essentially complex configurations). The assessments need to include the absolute values of forces and moments as well as the various symmetric and asymmetric stability derivatives, both steady and unsteady. A UCAV needs to be as light and small as possible for a given mission flight envelope. It is a compromise between efficient high-speed flight, loiter and good stability and handling at low speeds. A UCAV need to be as light and small as possible for a given mission flight envelope. It is a compromise between efficient high-speed flight, loiter and good stability and handling at low speeds.
We look at a planar wing (P0) and two designs: a notional intuitive design (BG2) and a modal "compromise" design (C1) enabling low and high speed flight. Figures presented illustrate the essential features and differences e.g. on spanwise and chordwise loadings at low and high speeds

Low speed experimental data is available on the BG2 wing model tested by DLR.

Results are compared with BG2 experiment and CFD RANS methods utilizing structured (ENSOLV, NLR) and unstructured (EDGE, FOI) grids. The emphasis is on symmetric longitudinal stabilitys.

It is inferred that CFD reflects the main charyacter of the BG2 wing and that the behaviour of the designed UCAV wing (C1) in reality can be predicted well byCFD.

The work so far has been interesting and encouraging. It has led to an improved understanding of the complex configurations with strongly interacting and separating / moderate sweep vortical flows.

In the wider perspective, for future, an understanding has evolved for either exploitation or avoidance of the complex flows. This is an important motivation.

1. INT RODUCTION

Work is being conducted under the NATO RTO-AVT-161 Task group on assessment of Stability and Control Prediction Methods for Air and Sea Vehicles (essentially complex configurations). See Refs.1-5. The assessments need to include the absolute values of forces and moments as well as the various symmetric and asymmetric stability derivatives, both steady and unsteady. This paper relates to the UCAV wing (termed SACCON) design aspects. A UCAV needs to be as light and small as possible for a given mission flight envelope. It is a compromise between efficient high-speed flight, loiter and good stability and handling at low speeds.

Results of an experimental test series have been published in Ref.3. The results included valuable data on forces, moments and pressures etc.

These aspects and our previous experience, presented an important opportunity for verification of our predictive methods (e.g. Refs.6-14, using a combination of linear, panel and Euler codes) and a useful starting point for the design process for "tolerant" wing designs (biased more towards low-speed, high lift).

The philosophy followed has to compare predictions with existing information on planar wings. With this confidence, we can then design more easily with different constraints.

We consider 3 wings: a planar uncambered one (P0) and two designed wings: a notional "intuitive" design (BG2, SACCON adopted by the Task group) and a new modal "compromise" design (C1).

Wing Geometry & Flight Envelope

Fig.1 shows the lofting of the UCAV wing. Pertinent data on the wind tunnel model is in **Table 1** (see Ref.3).

Figs.2-3 show typical flight envelope considerations. Although designed for "best cruise" (Mach, wing loading and CL), Take-Off , loiter and Landing conditions must also be accommodated.

Fig.4 shows the inverted 10% model, mounted from above, in the DNW Low-Speed Wind-Tunnel Braunschweig (DNW-NWB). The mounting allows for steady and unsteady measurements to be made.

To make the design and analysis process understandable, we need a reference uncambered wing planform. The main emphasis is on longitudinal stability aspects. Refs.11-13 show examples of our previous wing design work, showing a combination of codes: linear, panel, Euler and RANS.

2. UNCAMBERED WING P0

The wing planform has a continuous LE with +53^o sweep. The TE is cranked at 29% and 77% semi-span resulting in inner, mid and outer TE sweeps of -53^o, +53^o and -53^o respectively. Aerofoil section and panel distributions are shown in **Fig. 5** together with t/c and r/c spanwise distributions. Typical Wind Tunnel model cambered sections are also shown.

Fig. 6 shows the spanwise loadings and chordwise pressure distributions at Mach 0.75. Possible cruise CL occurs at 4^o < AoA < 5^o. Tip loadings are extremely high, indicating flow separation. Spanwise loadings and pressure distributions are shown in **Fig. 7** for Mach 0.2. Again the tip loadings are extremely high in the required CL range, 0.6 to 0.8. AoA requirements are also very high, 12^o to 16^o.

The low and high speed results indicate the need for camber and twist to achieve a practical design.

3. NOTIONAL "INTUITIVE" UCAV WING DESIGN BG2

The BG2 (Notional Wing Design) section distribution is compared with the uncambered case in **Fig. 8**. Wing twist (LE down) is evident, starting at the inner crank and increasing towards the tip. The spanwise loadings and chordwise pressure distributions at Mach 0.75 are shown in **Fig. 9**. The LE suctions have been ameliorated to a large extent although the tip remains heavily loaded at cruise CL (0.28, AoA 5.57^o). **Fig. 10** shows the spanwise loadings and chordwise distributions at Mach 0.2. In the required CL range, the tip is again heavily loaded indicating that further design improvements are required.

4. DESIGNED UCAV WING C1

A suitable wing design will incorporate sufficient twist to "contain" the tip flow at high and low speeds to prevent flow separation and pitch-up. This could be achieved by imposing "wash-out" over the tip region to ensure that local lift remains at zero or slightly negative. This needs to be finely tuned via a modal process minimizing drag penalties whilst ensuring lift demands on the inner wing are not excessive.

A designed UCAV wing (C1) section distribution is compared with the uncambered P0 case in **Fig. 11**. A high degree of twist (LE down) dominates the tip region. The inner region exhibits positive twist. The spanwise loadings and chordwise pressure distributions at Mach 0.75 are shown in **Fig. 12**. Over a typical design CL range (0.22 to 0.34) the tip region remains negatively loaded. **Fig. 13** shows the spanwise loadings at Mach 0.2 and predicted, attached flow pressure distributions at required CL are shown in **Fig. 14**. **Fig. 15** compares the P0, C1 and BG2 Mach 0.2 Cp distributions at CL = 0.36. Composite Cp contours and streamlines for BG2 (Euler CFD, Ref.14) are also shown. Note the Cp behaviour near the tip. At AoA 7^o, the tip of C1 remains negatively loaded. A further increase in AoA would result in onset of flow separation and vortical flow. This is evident in the Cp distributions of BG2 at the same CL.

5. COMPARISONS, CFD RESULTS & EXPERIMENT

Two CFD RANS codes have been used: structured code ENSOLV (NLR) and unstructured code EDGE (FOI) and results have been presented in **Figs.16-24**.

Experimental data on the model BG2 has been provided from the DNW low speed wind tunnel tests carried out at a nominal airspeed of 60 m/s (maximum 75 m/s). Assuming atmospheric conditions at Sea Level, 60 m/s corresponds to Mach 0.176. The Reynolds number is 1.93 x10^6, based on model aerodynamic chord.

Fig. 16 compares the streamlines and vorticity distributions on wings BG2 and C1, using EDGE. Note that at a given nominal AoA, the wing BG2 has about 0.04 to 0.05 less CL than wing C1 (See **Figs. 19 & 21**) so the lift levels are not identical in the comparisons. We note that vorticity generated by C1 in AoA range 15-21 is substantially less "distributed" (colourful !). That would indicate less perturbed flow.

For wing BG2, AoA 5.36, 7.46, 10.63, 12.76 and 14.88, **Fig. 17** compares the Cp distributions (constant x stations), experiment and ENSOLV. The simulations were performed on a multi-block structured grid with 6.973,440 grid cells and 1000 iterations were needed for converged solutions. Results for two wind tunnel test runs (TN2373 VN1001 and VN1002) using the same conditions are shown. Note that in the experimental data shown boundary layer trips are not present. The various sections are as shown in the inset figure (top right), K/C varies from 0 to 1 = centreline to tip. Note that agreement between theory and experiment is very reasonable and encouraging at all AoA.

For wing BG2, **Fig. 18** compares the forces and moments from experiment and the two CFD codes: ENSOLV, EDGE.

From these results it can be inferred that CFD codes encouragingly reflect the main character of the BG2 wing. However, there are some reservations. Experimental results show higher CLmax and higher L/D. The drag values are slightly higher for CFD. In a "real application", there would be other drag contributions e.g. due to propulsion integration etc. that will increase the drag further. The experiment shows a pitch-down tendency at AoA about 10^o, CL near 0.45. The ENSOLV code reflects similar tendency at AoA 12.5^o. The EDGE code although showing a more positive Cm slope, has a similar (gentler) tendency at AoA 12.5^o.

We can mention that such encouraging correlations between experiment and theory provide adequate confidence for the design work. We now show further comparisons for BG2 and C1 at low and high speeds.

BG2 and C1 Comparisons at Low speed, Mach 0.17

Using ENSOLV, **Fig. 19 & 20** refer to comparison at Reynolds number of 1.93 x 10^6 and 19.3 x 10^6 respectively. The Wing C1 shows lower drag at higher CL values. There are no significant changes in character due to Reynolds numbers increasing. Slightly higher L/D values are shown at the higher Reynolds number.

Using EDGE, **Fig. 21** shows comparisons at Reynolds number of 1.93 x 10^6. This confirms the lower drag for C1 at

higher CL values and emphasises that higher CLmax is attained with wing C1.

BG2 and C1 Comparisons at High speed, Mach 0.75

There is no experimental data at high speed. The results (theory) give an idea of the likely comparative behaviour for the two wings. Using ENSOLV, **Fig. 22 & 23** refer to comparison at Reynolds number of 1.93 x 10^6 and 19.3 x 10^6 respectively. .Using EDGE, **Fig. 24** shows comparisons at Reynolds number of 1.93x10^6.

At the flight-realistic case, with higher Reynolds number, there are no significant differences in L/D at CL near 0.25. For the more academic lower Reynolds number case, EDGE results show a slightly lower L/D values for wing C1, but ENSOLVE does not reflect this.

For Wings BG2 and C1, using EDGE Euler mode, **Figs.25 & 26** show the Mach number and Cp contours at AoA 5 deg. (upper and lower surfaces) Essentially, the flow patterns look very similar. No build up of shocks is noted. However, at AoA 6.6 deg., the BG2 wing (composite picture, wakes and Cp contours) shows a shock build up. Further details are in Ref.14.

Summarising, the low speed comparisons, the wing C1 demonstrates a very significant improvement over the wing BG2. At transonic speed flight, the wing C1 performance is similar to that for the wing BG2. With no significant penalty at transonic speeds, we can infer that the wing C1 can be further enhanced / optimised.

6. CONCLUDING REMARKS & GENERAL INFERENCES

This paper is via the initiative of the NATO RTO-AVT-161 Task Group. The group is aimed at the assessment of Stability and Control Prediction Methods for the NATO Air and Sea Vehicles (essentially complex configurations). The assessments need to include the absolute values of forces and moments as well as the various symmetric and asymmetric stability derivatives, both steady and unsteady.

This paper relates to the UCAV wing design aspects. For a given mission flight envelope, a UCAV needs to be as light and small as possible. It is a compromise between efficient high-speed flight, loiter and good stability and handling at low speeds.

We considered three wings, a planar uncambered one (P0), a notional “intuitive” design (BG2) and a modal “compromise” design (C1).

Low speed experimental data is available on the BG2 wing model tested by DLR. These results have been compared with two RANS CFD codes: structured code ENSOLV (NLR) and unstructured code EDGE (FOI). The emphasis has been on longitudinal stability aspects. The encouraging correlations between experiment and theory for the wing BG2 has provided adequate confidence for the design work and evaluation of C1.

At low speeds, the wing C1 demonstrates a very significant improvement over the wing BG2. At transonic speed flight, the wing C1 performance is very similar to that for the wing BG2. In light of no significant penalty at transonic speeds, we can infer that the wing C1 can be further enhanced / optimised.

In the wider perspective for future, an understanding has evolved for either exploitation or avoidance of the complex flows on UCAV wings. This is an important motivation.

7. ACKNOWLEDGEMENTS

This work is part of current in-house R & D activities. Nevertheless it has been a sizeable undertaking, all in the cause of science! The authors have pleasure in acknowledging work of DNW in supplying Wind Tunnel results and helpful discussions with Dipl. -ing. Andreas Schuette. Thanks are due to Dr. M.E. Palmer for his patient technical assistance. Any opinions expressed are those of the authors. The authors have been privileged to be members of AVT-161 task group. It is felt that the Task group work has been truly inspirational and thorough, being accomplished by motivated and expert researchers. Opportunities for future collaboration are warmly invited.

REFERENCES

1. Report for AVT-161 Task Group, with contributions from several authors, including the present authors.
2. CUMMINGS, R, SCHEUTTE, A., “An Integrated Computational/Experimental Approach to UCAV Stability & Control Estimation: Overview of NATO RTO AVT- 161”, AIAA-2010-4392.
3. LOESER, T., VICROY, D. & SCHUETTE, A., “SACCON Static Wind Tunnel Tests at DNW- NWB and 14´x22´ NASA,LaRC”, AIAA-2010-4393.
4. TORMALM, M., TOMAC., M & SCHMIDT, S., “Computational Studies of Static and Dynamic Vortical Flow over SACCON Configuration using the FOI solver Edge”, AIAA-2010-4561.
5. RIZZI, A, TOMAC, M & NANGIA, R., ”Engineering methods for SACCON configuration”, AIAA-2010-4398.
6. NANGIA, R.K. & PALMER, M.E., "Application of Subsonic First-Order Methods for Prediction of Inlet & Nozzle Aerodynamic Interactions with Airframe", Symposium on "Aerodynamic Engine/Airframe Integration for High Performance Aircraft & Missiles", Fort Worth, Texas, USA, AGARD CP-498, 1991.
7. NANGIA, R. K., "Low Speed Performance Optimisation of Advanced Supersonic Civil Transport with Different LE & TE Devices", EAC'94, Toulouse, France, October 1994.
8. NANGIA, R.K. & MILLER, A.S., "Vortex Flow Dilemmas & Control on Wing Planforms for High Speeds", Paper Presented at RTO - AVT Symposium, Loen, Norway, May 2001.
9. NANGIA, R.K., "Semi-Empirical Prediction of the Vortex Formation on the VFE-2 Configuration (65 deg. Delta Wings with different Leading Edge shapes)”, Chapter 33, RTO-AVT-113 Report, Formal Publication 2008.
10. NANGIA, R.K., "Semi-Empirical Prediction of the Vortex Onset & Progression on 65 deg. Delta Wings (RTO-AVT-113, VFE-2 Facet) ”, 46th AIAA Aerospace Sciences. Meeting, Reno, AIAA-2008-0384, January 2008.
11. NANGIA, R.K. & PALMER, M.E., “A Comparative Study of Several UCAV Type Wing Planforms – Aero Performance & Stability Considerations”, Paper AIAA-2005-5078, 23rd Applied Aerodynamics Meeting, Toronto, Canada, June 2005.

12. NANGIA, R.K., PALMER, M.E., "A Comparative Study of Four UCAV Wing Layouts – High-Speed Aero Performance & Stability Considerations", ICAS –2006-1.7, Hamburg, Sept 2006.

13. NANGIA, R.K., "Morphing Wings Incorporating In-Plane & Folded-Tips – "Inverse" Aerodynamic Design Studies" Paper for RTO-AVT 168, Lisbon, April 2009.

14. TOMAC, M., RIZZI, A., NANGIA, R.K., MENDENHALL, M.R. & PERKINS, S.C., Jr., "Engineering Methods on the SACCON con_guration - Some Design Considerations", AIAA-2010-4398, June 2010.

NOMENCLATURE

AR Aspect Ratio
b = 2 s, Wing span
c Local Wing Chord
c_{av} = S/b, Mean Geometric Chord
c_{aero} = c_{ref} = Mean Aerodynamic Chord of Wing
C_A = Axial force/(q S), Axial Force Coefficient
C_{AL} Local Axial Force Coefficient
C_D = Drag Force /(q S), Drag Coefficient (C_{Di}+ C_{D0})
C_{Di} Lift Induced Drag Coefficient
C_{DL} Local Drag Coefficient
CG Centre of Gravity
C_l = Rolling Moment/(qSs), Roll Moment Coefficient
C_L = Lift Force/(q S), Lift Coefficient
C_{LL} Local Lift Coefficient
C_m = m/(q S c_{aero}), Pitching Moment Coefficient
C_{mL} Local Pitching Moment Coefficient
C_n = Yawing moment/(q S s), Yawing Moment Coefficient
C_P Coefficient of Pressure
C_Y = Side Force/(qS) ,Side-force Coefficient
ΔC_D Difference in C_D
LE, TE Leading Edge, Trailing Edge
L/D Lift to Drag ratio
m Pitching moment
M Mach Number
q = 0.5 ρ V^2, Dynamic Pressure
Re Reynolds Number, based on c_{aero}
s, S semi-span, Wing Area
S Wing Area, also Reference
V Free-stream Velocity
x, y, z Axes system of an aircraft
x_{AC} Chordwise position of Aerodynamic Centre
x_{CP} Chordwise location of Centre of Pressure
y_{CP} Spanwise location of Centre of Pressure
α AoA, Angle of Attack
ß Sideslip Angle
λ Taper Ratio, c_t/c_r
Λ LE Sweep Angle
η = y/s, Non-dimensional spanwise distance
ρ Air Density

Table 1 UCAV BG2 CONFIGURATION MODEL, DIMENSIONS & DEFINITIONS

	Model Metric	Units	Non-Dimensional Units Wing Semi-span = 1.0	
Wing Semi-span s	0.7688	m	1.0	
Wing Span b	1.5375	m	2.0	
Inner Wing Chord	1.0611	m	1.380217	
Wing Area S	0.7705	m^2	1.303776	
Standard Mean Chord c_{aero}	0.5012	m	0.651888	
Mach 0.2 NP x_{ac}	0.6013	m	0.782164	
Mean Aerodynamic Chord c_{aero}	0.479	m	0.623049	
Mean Aerodynamic Centre x_{ac}	0.6	m	0.7802	(CG location)

Copyright Statement

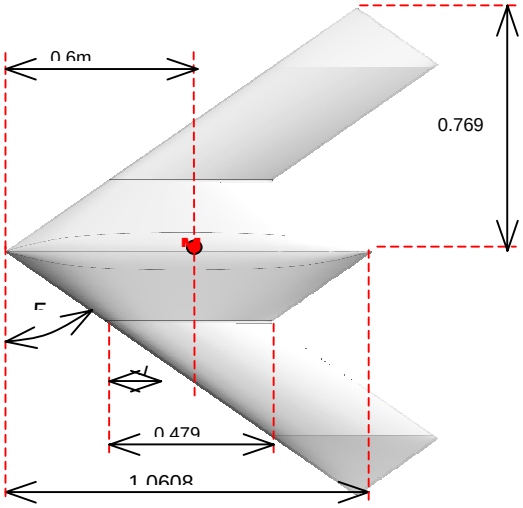

Fig. 1 LOFTING OF THE UCAV DESIGN

c_{ref} = 0.479m
MRP = 0.6m / 0.0m / 0.0m
S_{ref} = 0.77m^2 (full span model)

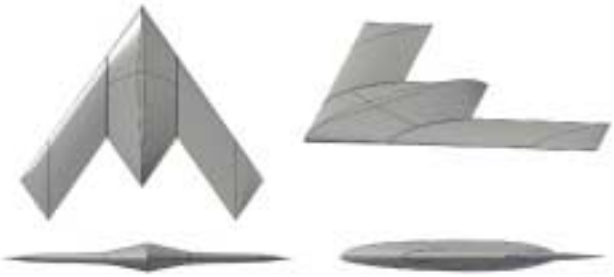

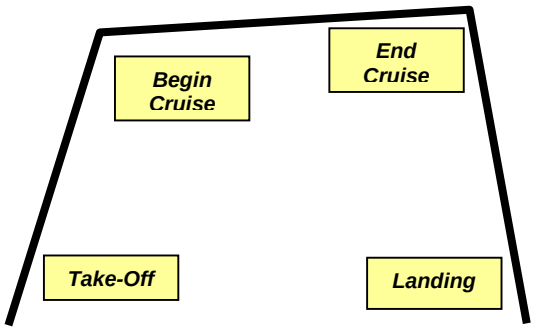

Take-Off W 26740 lb W/S 51 lb/ft^2
M 0.20 q 60 lb/ft^2 CL 0.84
M 0.25 q 92 lb/ft^2 CL 0.55

Start Cruise W 25500 lb W/S 48 lb/ft^2
M 0.80 q 176 lb/ft^2 CL 0.27

End Cruise W 15700 lb W/S 30 lb/ft^2
M 0.80 q 176 lb/ft^2 CL 0.17

Landing W 15120 lb W/S 29 lb/ft^2
M 0.20 q 60 lb/ft^2 CL 0.48

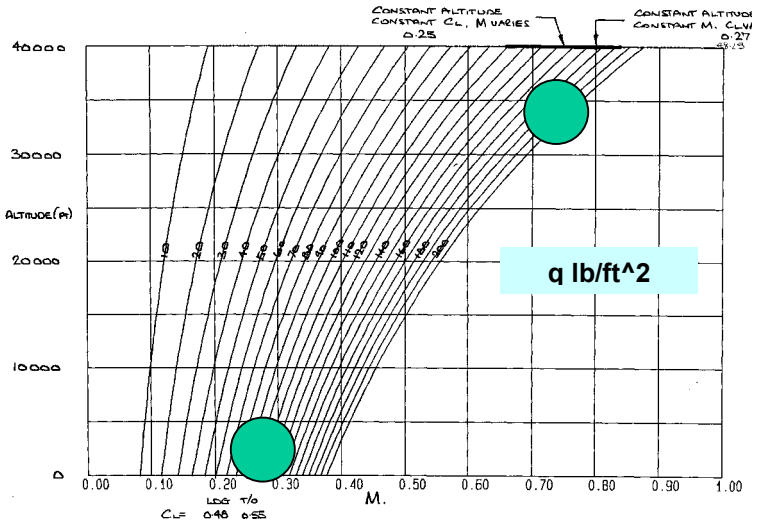

Fig. 2 FLIGHT ENVELOPE CONSIDERATIONS

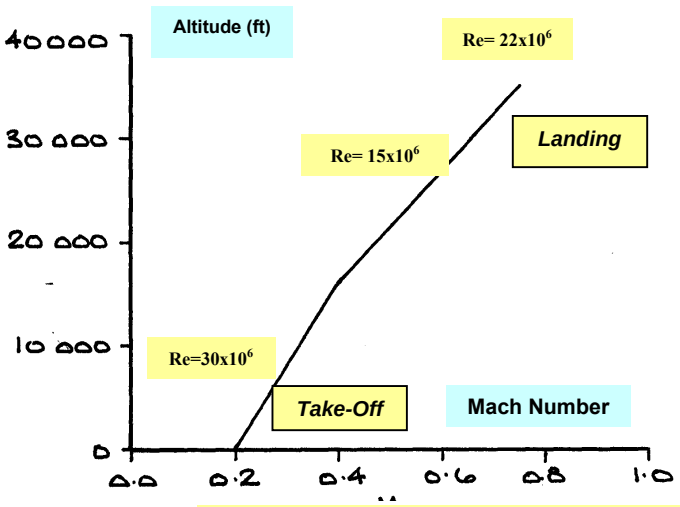

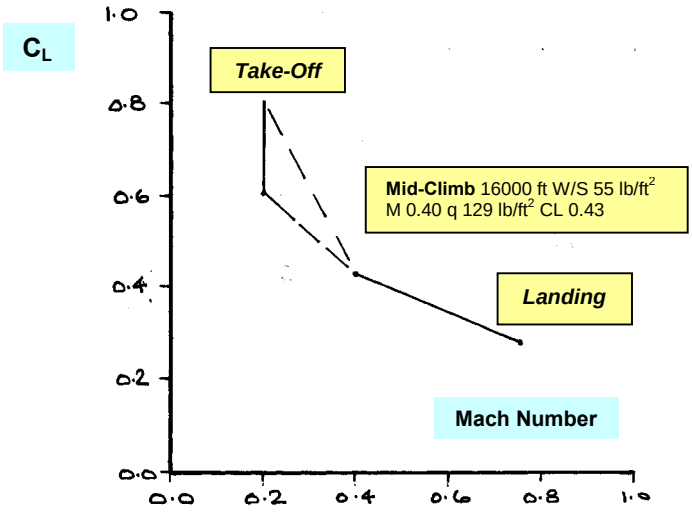

FIG. 3 FLIGHT ENVELOPE, ALTITUDE, C_L & MACH RELATIONSHIPS

Fig. 4 MODEL MOUNTED (UPSIDE-DOWN), DNW LOW-SPEED WIND-TUNNEL

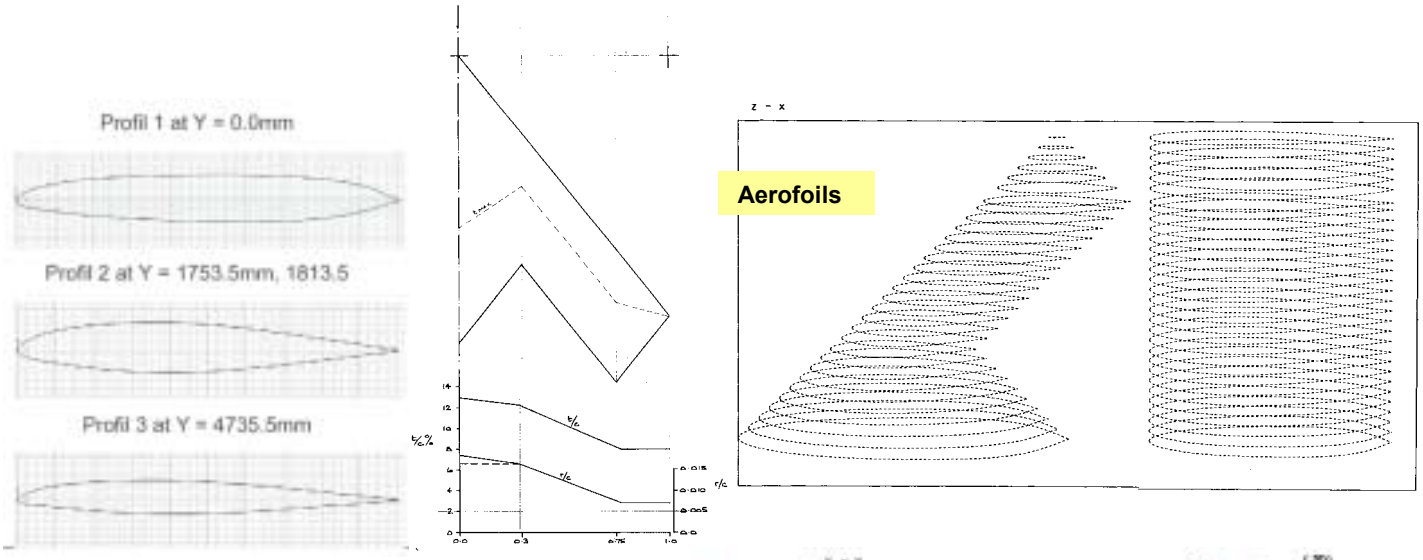

Wind Tunnel Model Aerofoil Sections (Cambered)

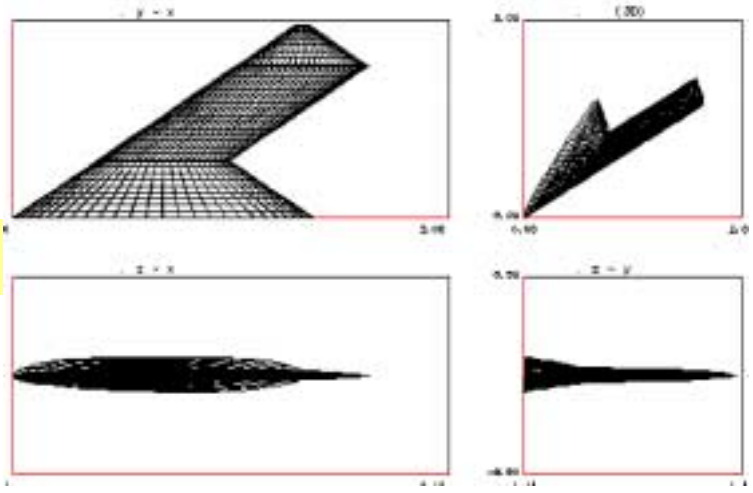

Fig. 5 UNCAMBERED WING P0, GEOMETRY, AEROFOILS & t/c, r/c VARIATIONS

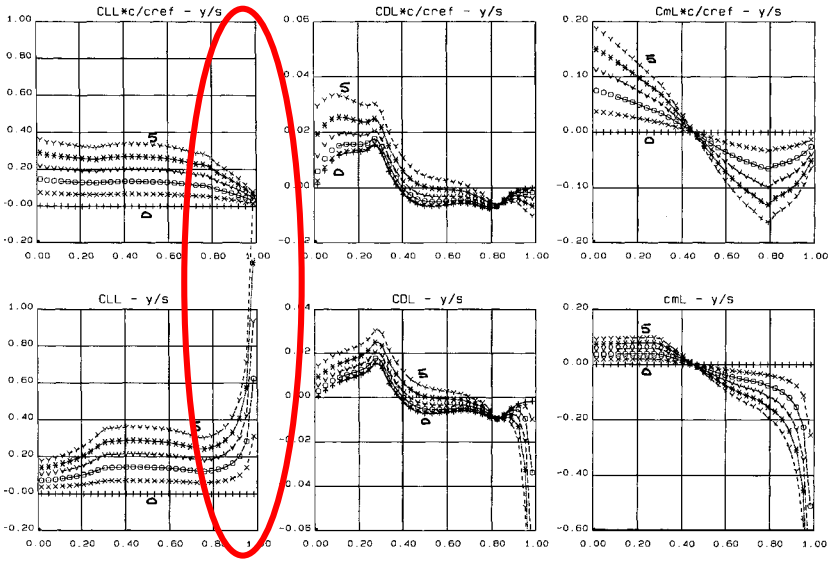

Spanwise Loadings

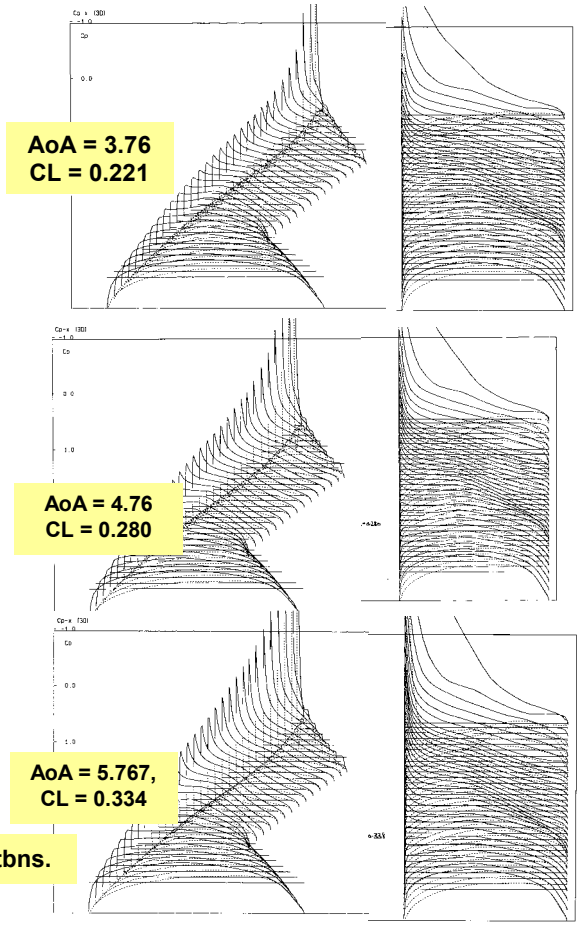

Cp Distbns.

FIG. 6 UNCAMBERED WING P0, Mach 0.75, CL, Cm & SPANWISE LOADINGS & Cp DISTBNS. Panel Code

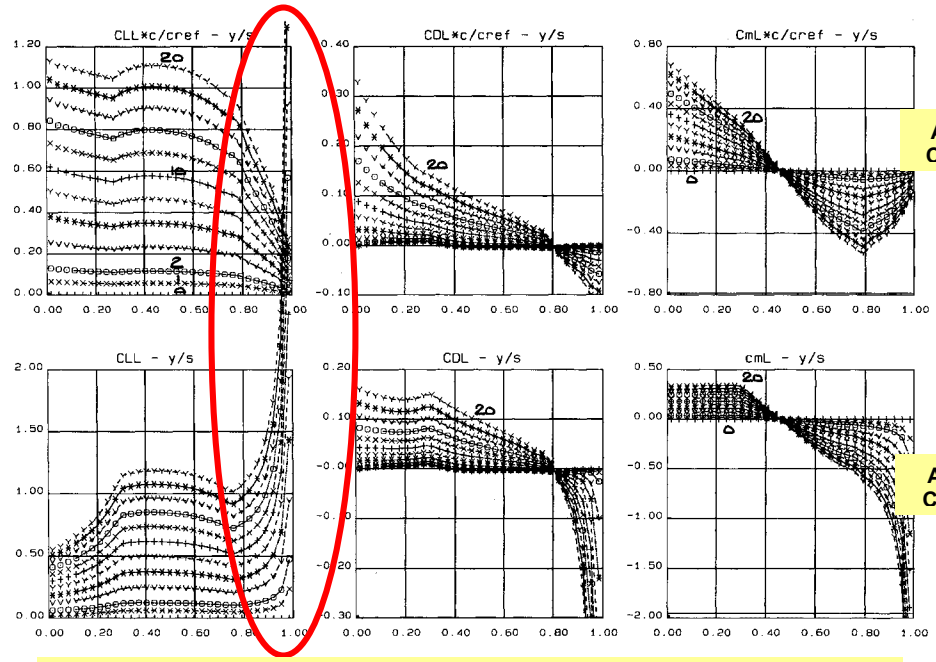

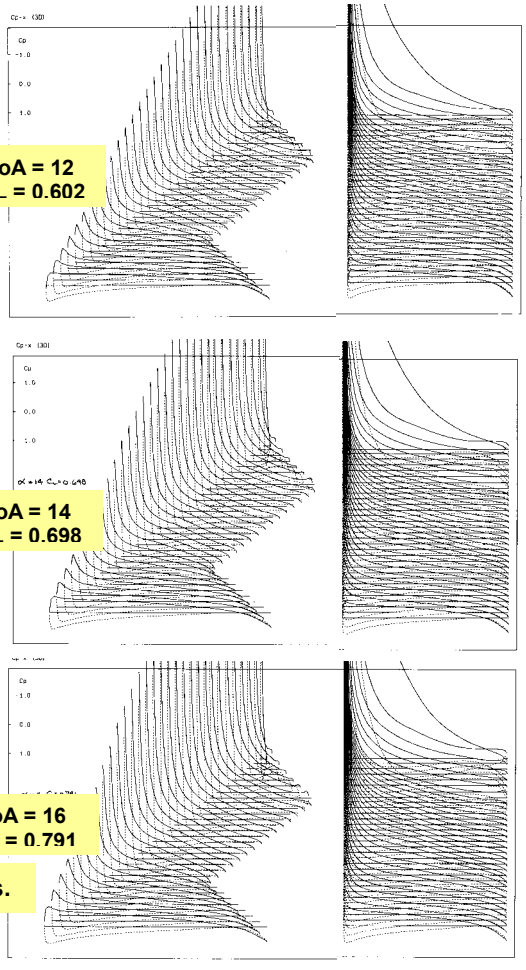

Cp Distbns.

FIG. 7 UNCAMBERED WING P0, Mach 0.2, SPANWISE LOADINGS & Cp DISTRIBUTIONS, Panel Code

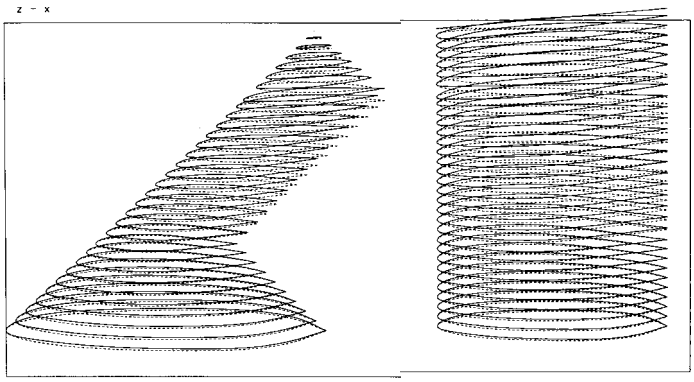

FIG. 8 COMPARING P0 & BG2 GEOMETRY

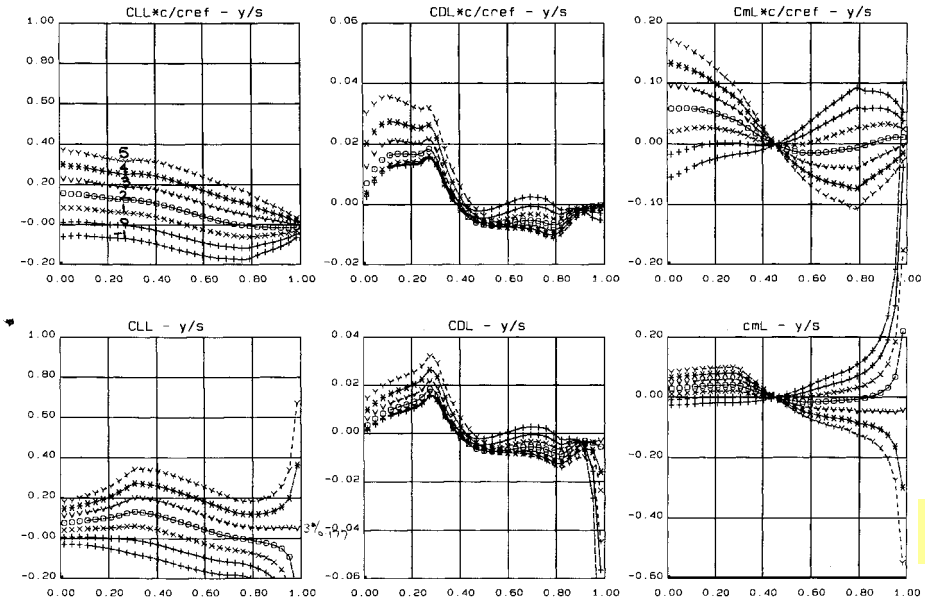

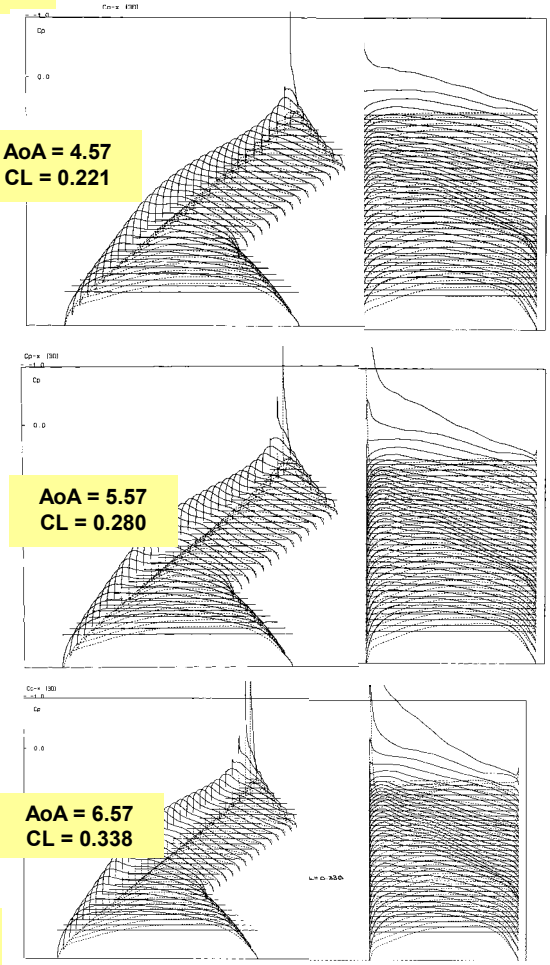

FIG. 9 BG2 WING, Mach 0.75, CL, Cm & SPANWISE LOADINGS, & Cp DISTRIBUTIONS, PANEL CODE

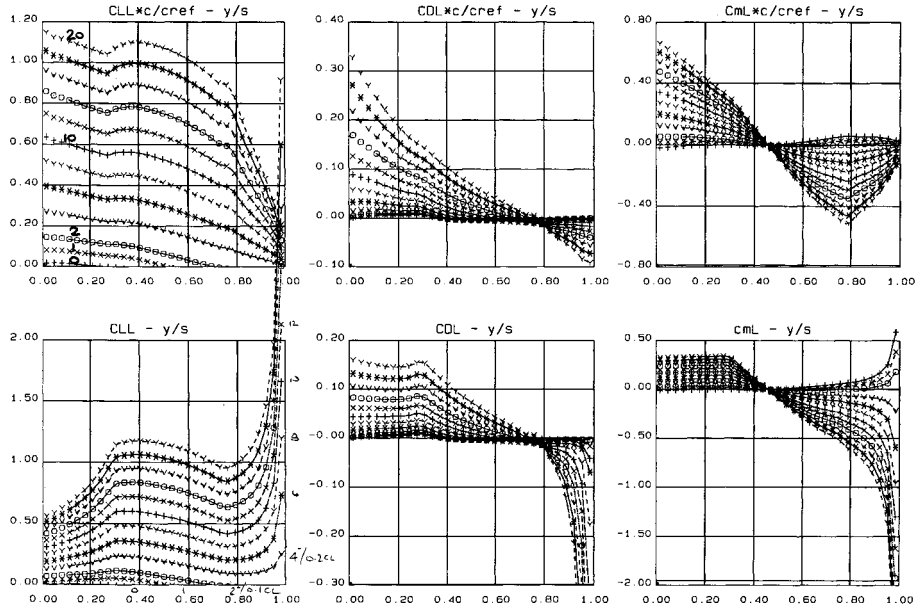

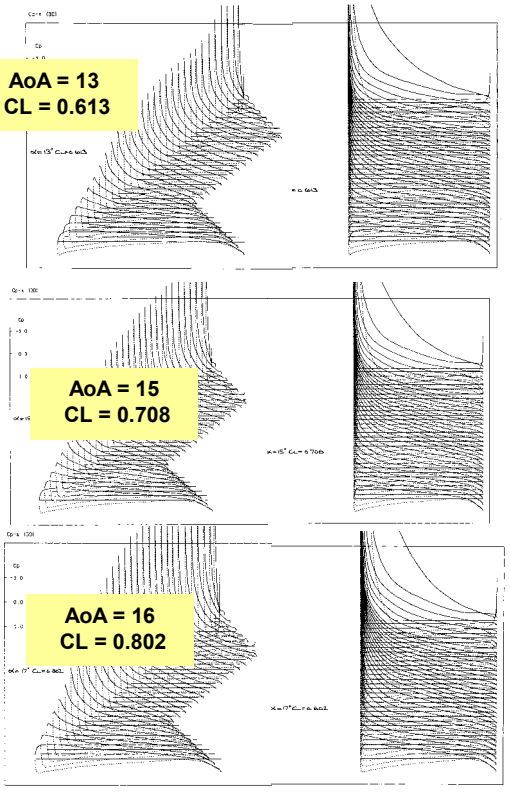

FIG. 10 BG2 WING, Mach 0.20, CL, Cm & SPANWISE LOADINGS & Cp DISTRIBUTIONS, Panel Code

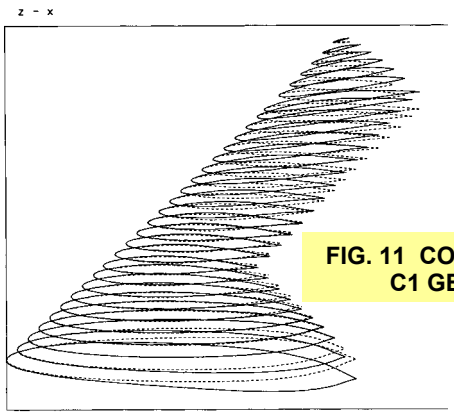

FIG. 11 COMPARING P0 & C1 GEOMETRY

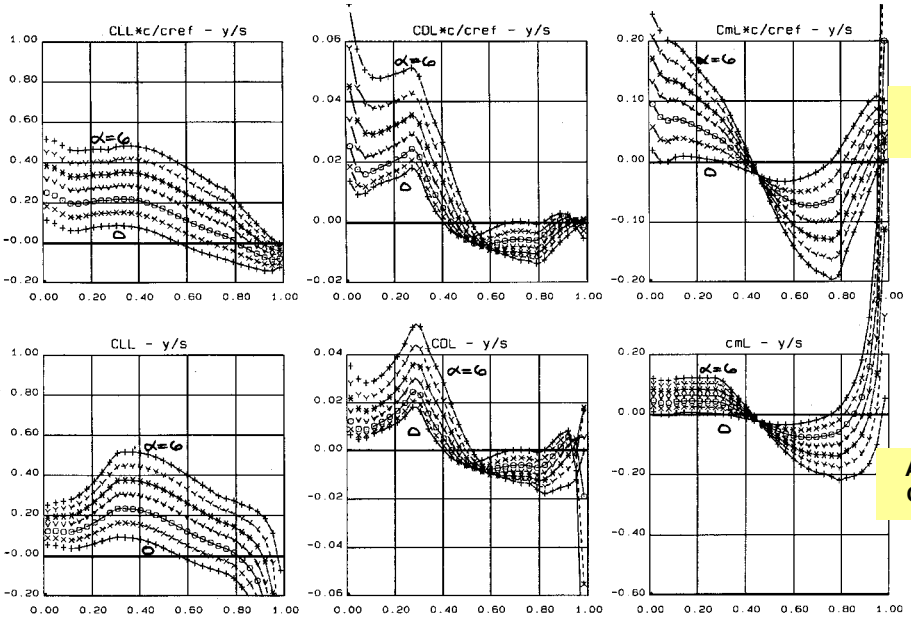

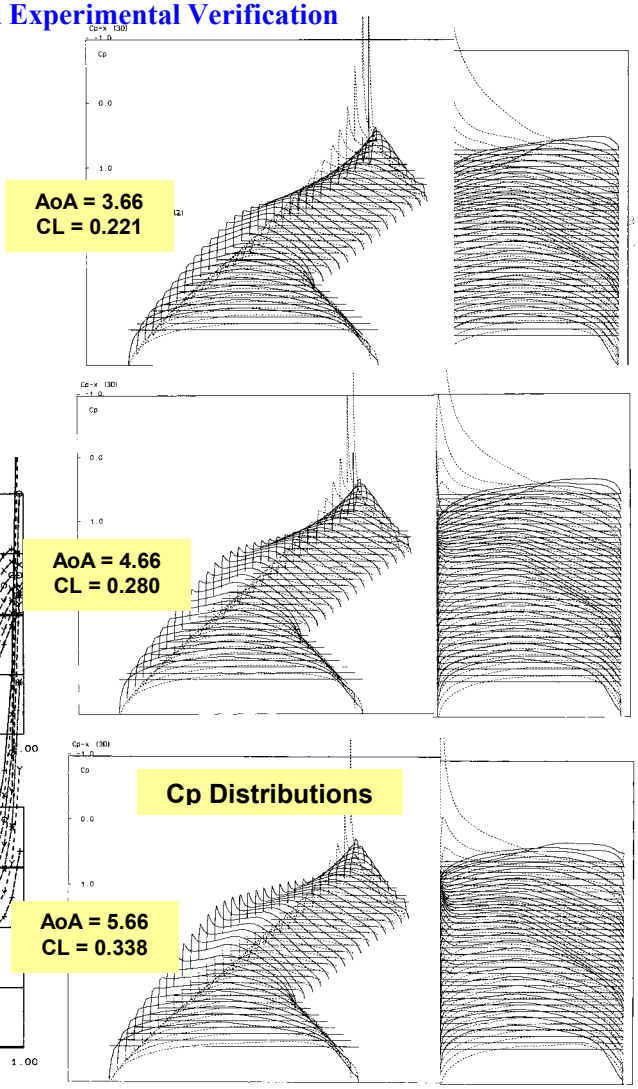

FIG. 12 C1 DESIGNED WING, Mach 0.75, CL, Cm & SPANWISE LOADINGS & Cp DISTRIBUTIONS, PANEL CODE

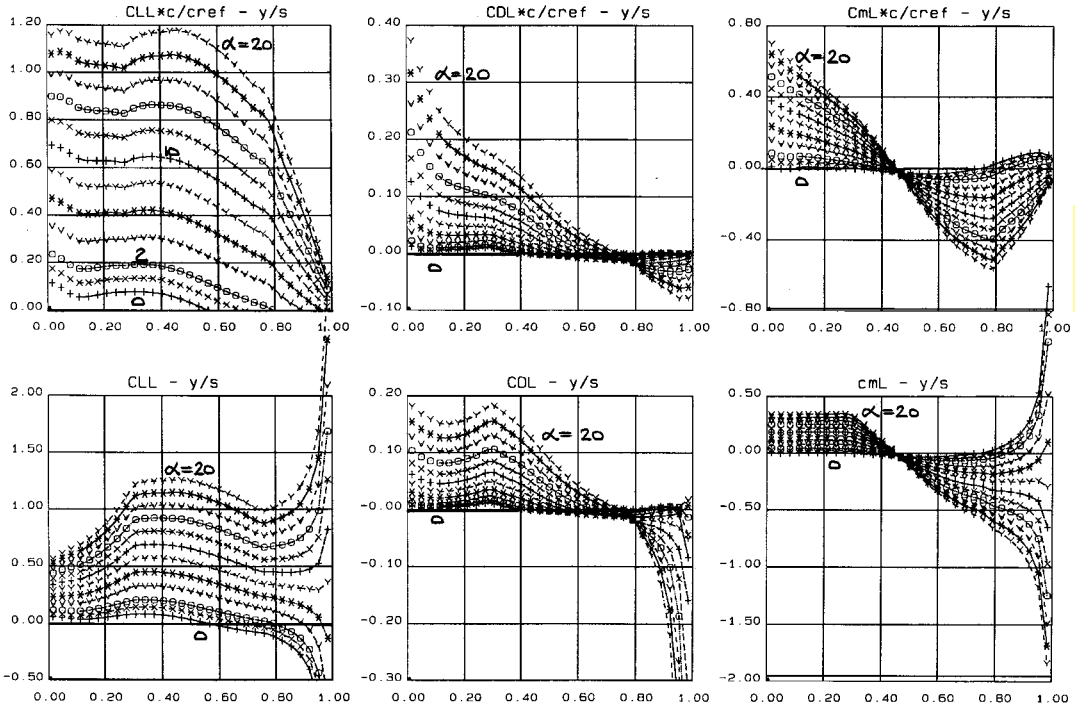

FIG. 13 C1 WING, Mach 0.2, CL, Cm & SPANWISE LOADINGS, Panel Code

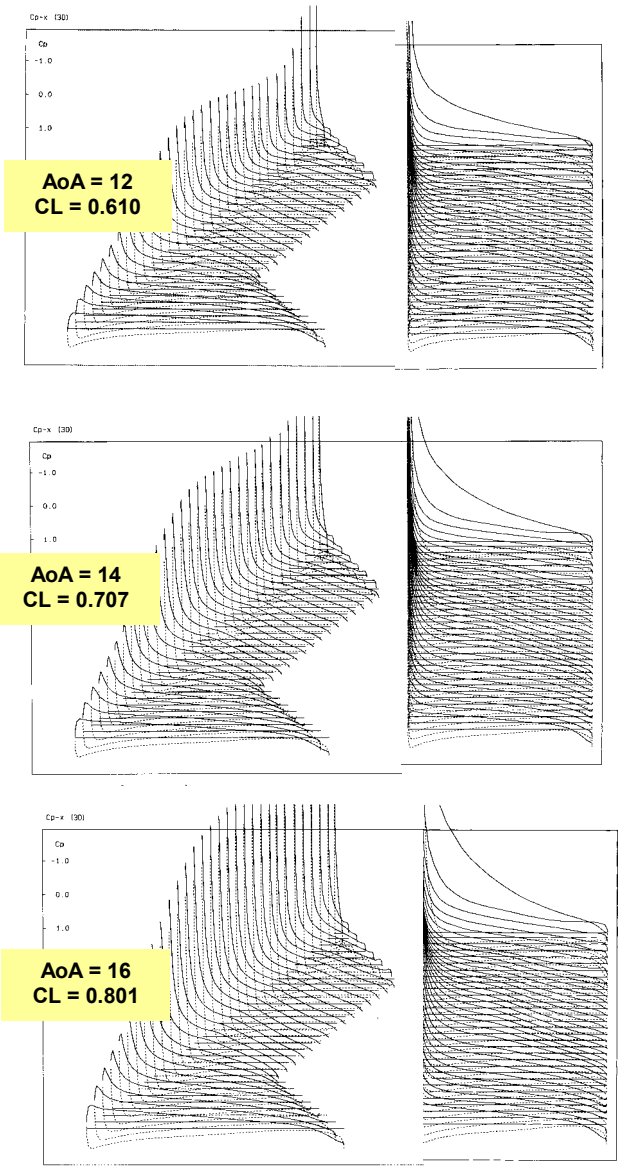

FIG. 14 C1 DESIGNED WING, Mach 0.2, Cp DISTRIBUTIONS

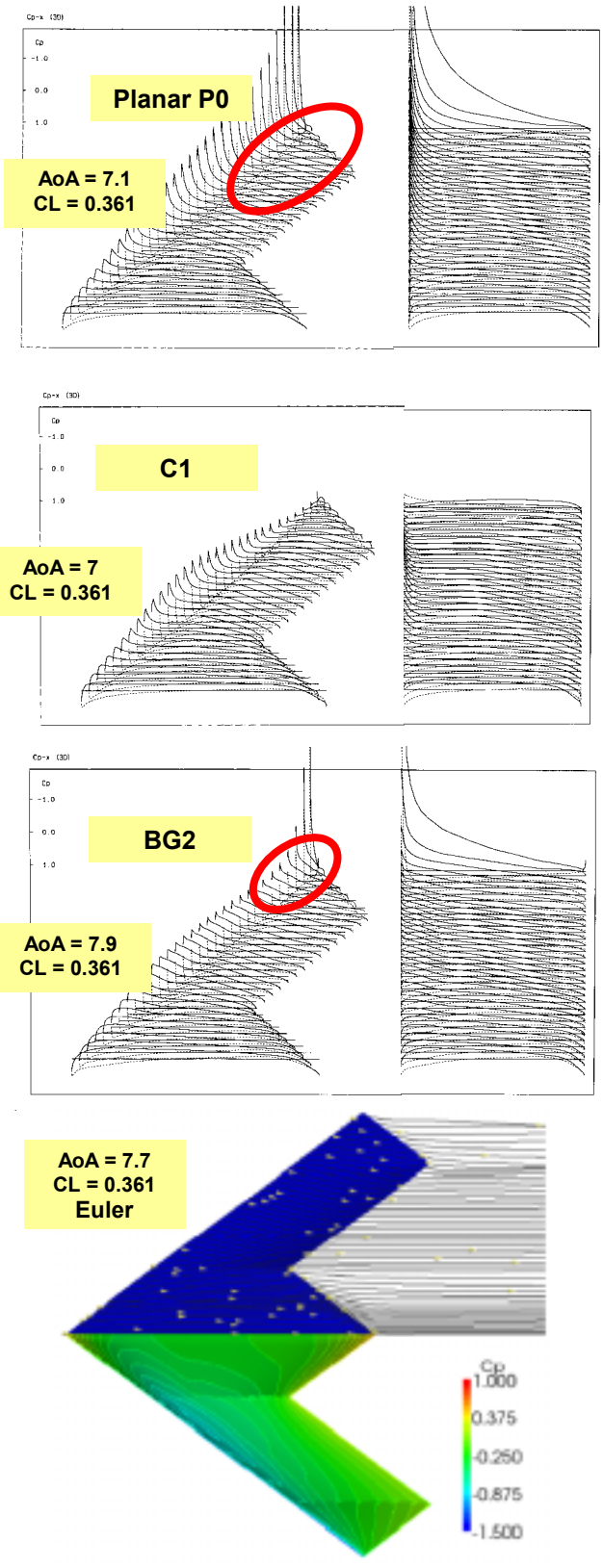

FIG. 15 ATTACHED FLOW Cp DISTRIBUTIONS NEAR ONSET OF VORTICAL FLOW ON C1 DESIGNED WING, Mach 0.2, CL = 0.361 COMPARED WITH Cp DISTRIBUTIONS ON P0 & BG2 AT CL = 0.361 (ASSUMING ATTACHED FLOW), IN REALITY, VORTICAL FLOW EXISTS

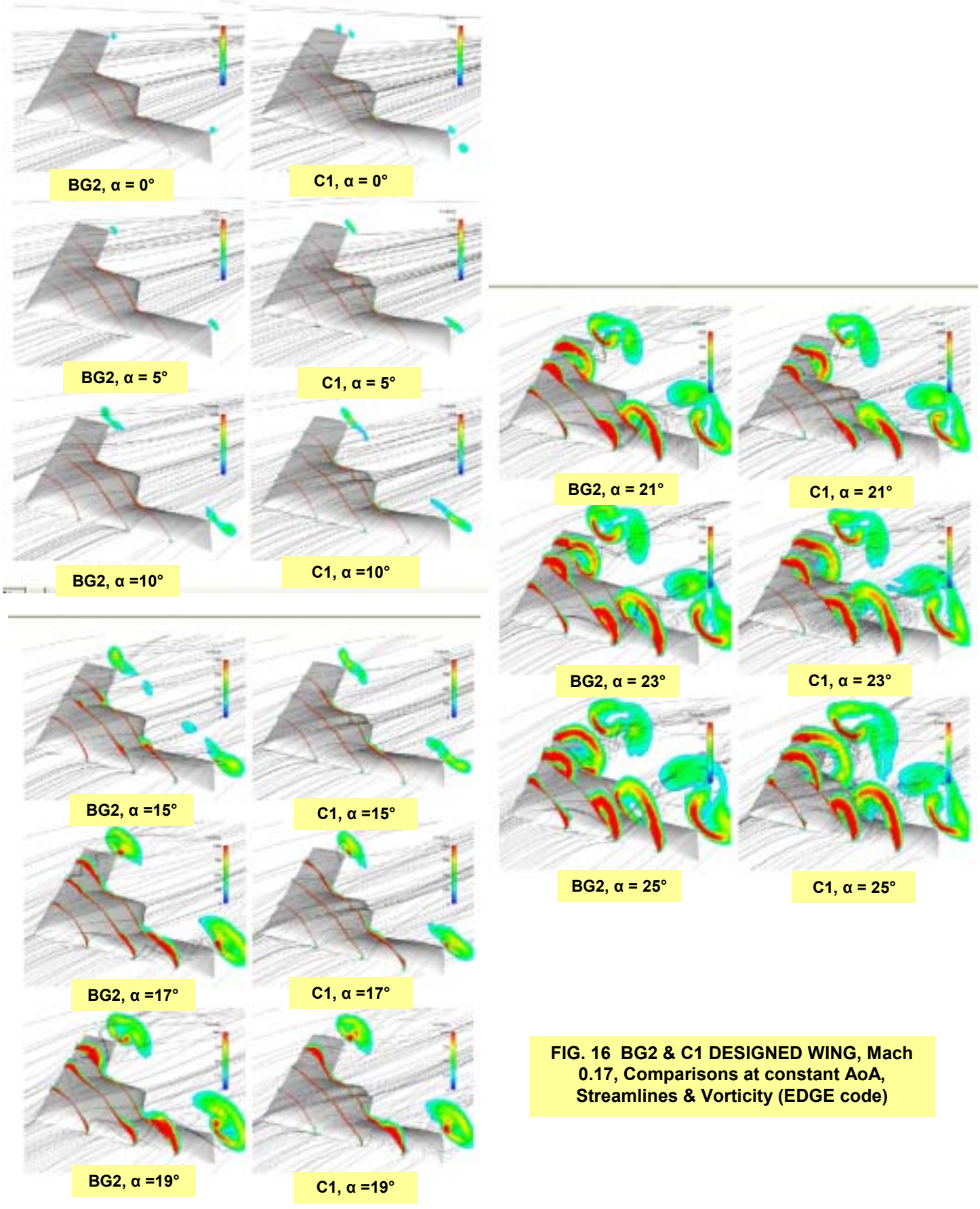

FIG. 16 BG2 & C1 DESIGNED WING, Mach 0.17, Comparisons at constant AoA, Streamlines & Vorticity (EDGE code)

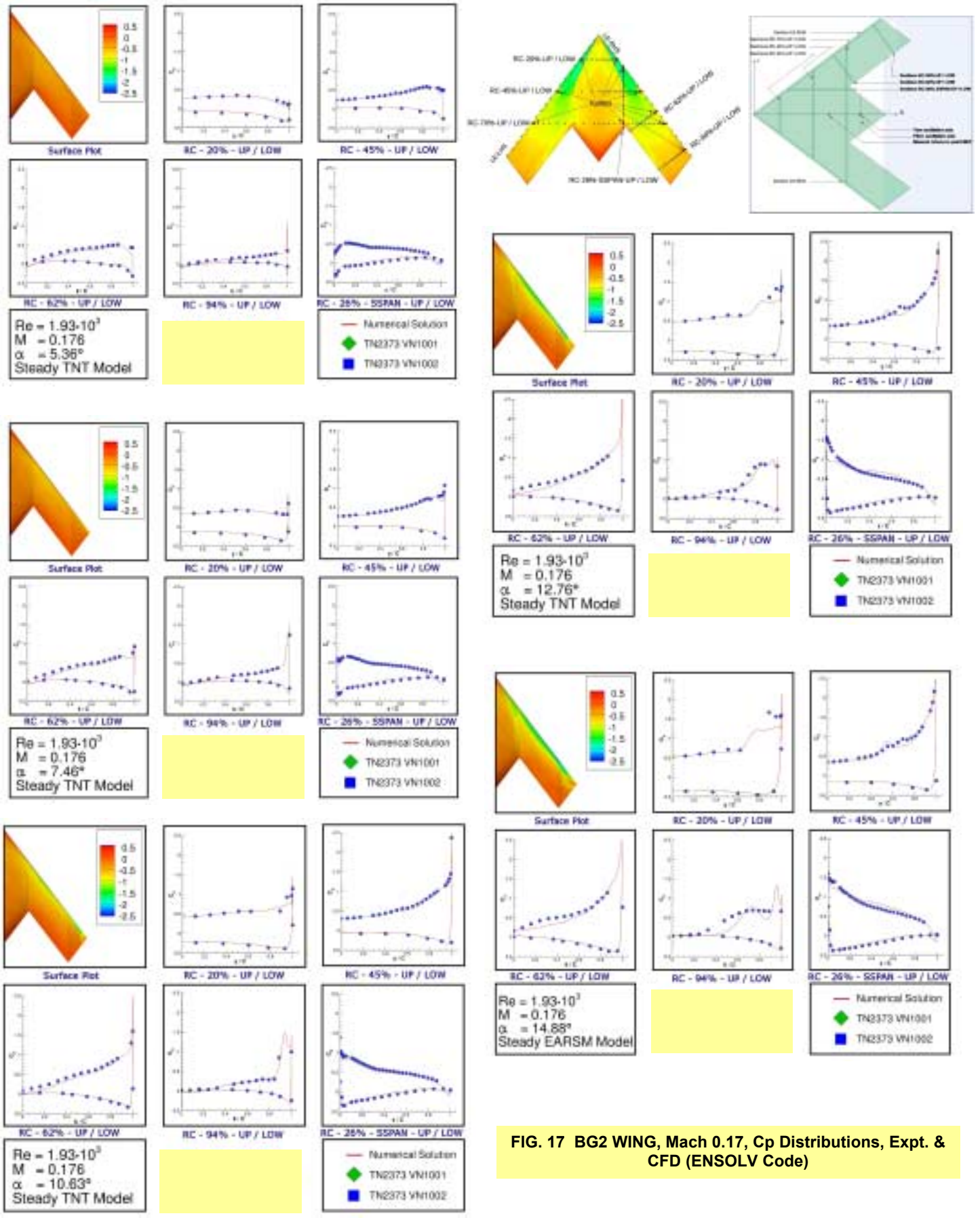

FIG. 17 BG2 WING, Mach 0.17, Cp Distributions, Expt. & CFD (ENSOLV Code)

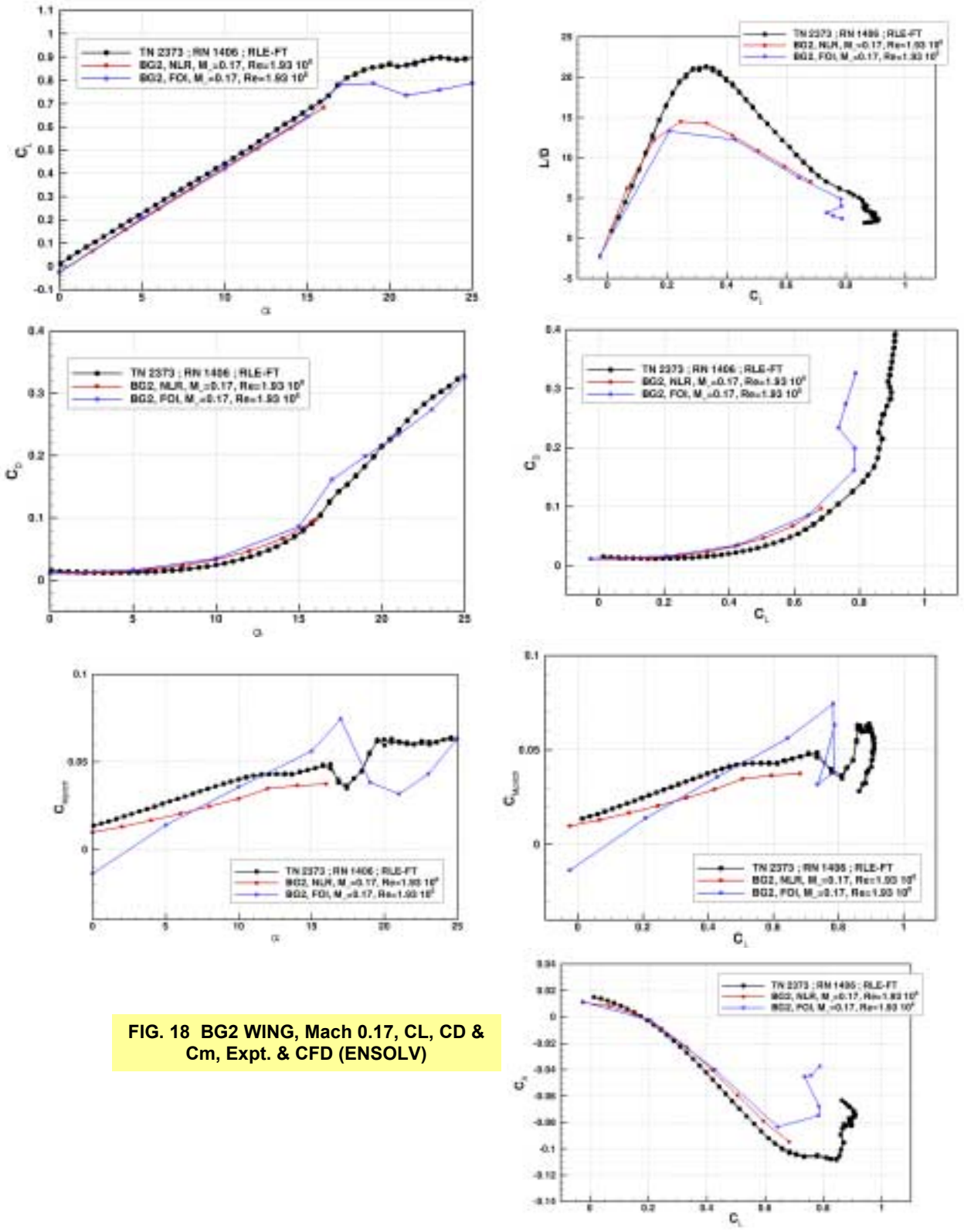

FIG. 18 BG2 WING, Mach 0.17, CL, CD & Cm, Expt. & CFD (ENSOLV)

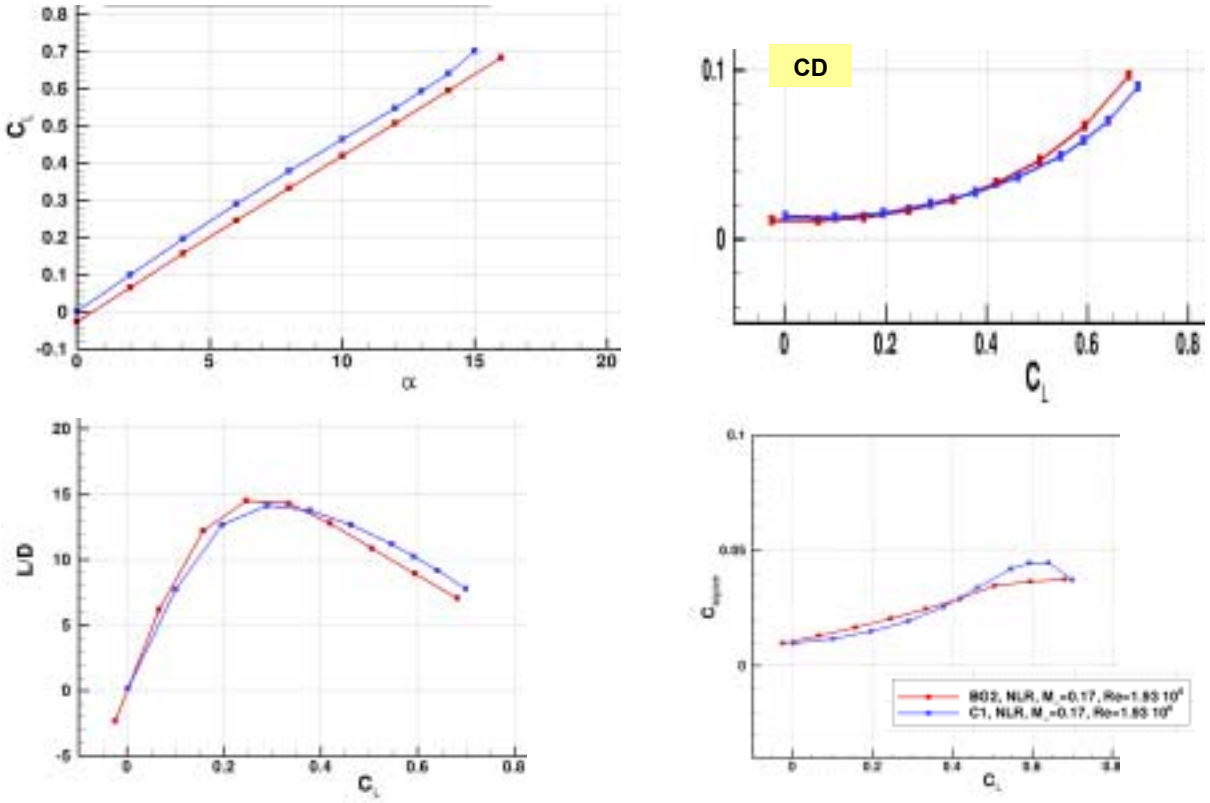

FIG. 19 BG2 & C1, Mach 0.17, Re=1.93x10^6 (ENSOLV)

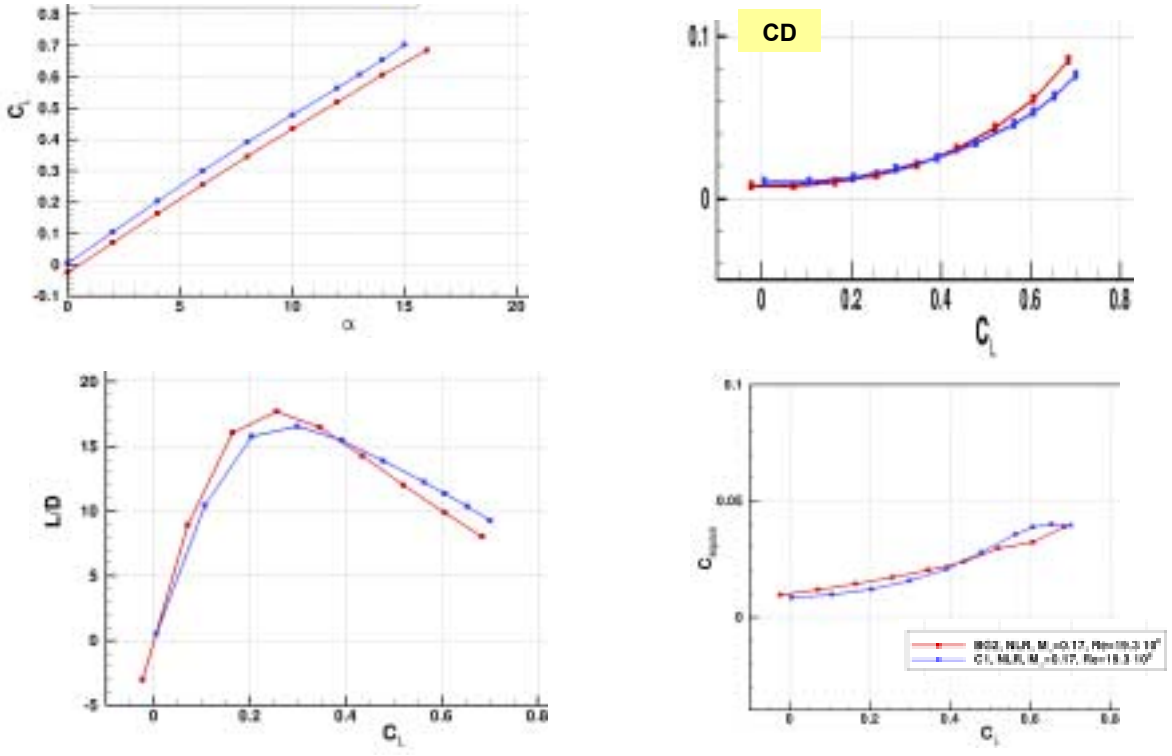

FIG. 20 BG2 & C1, Mach 0.17, Re=19.3x10^6 (ENSOLV)

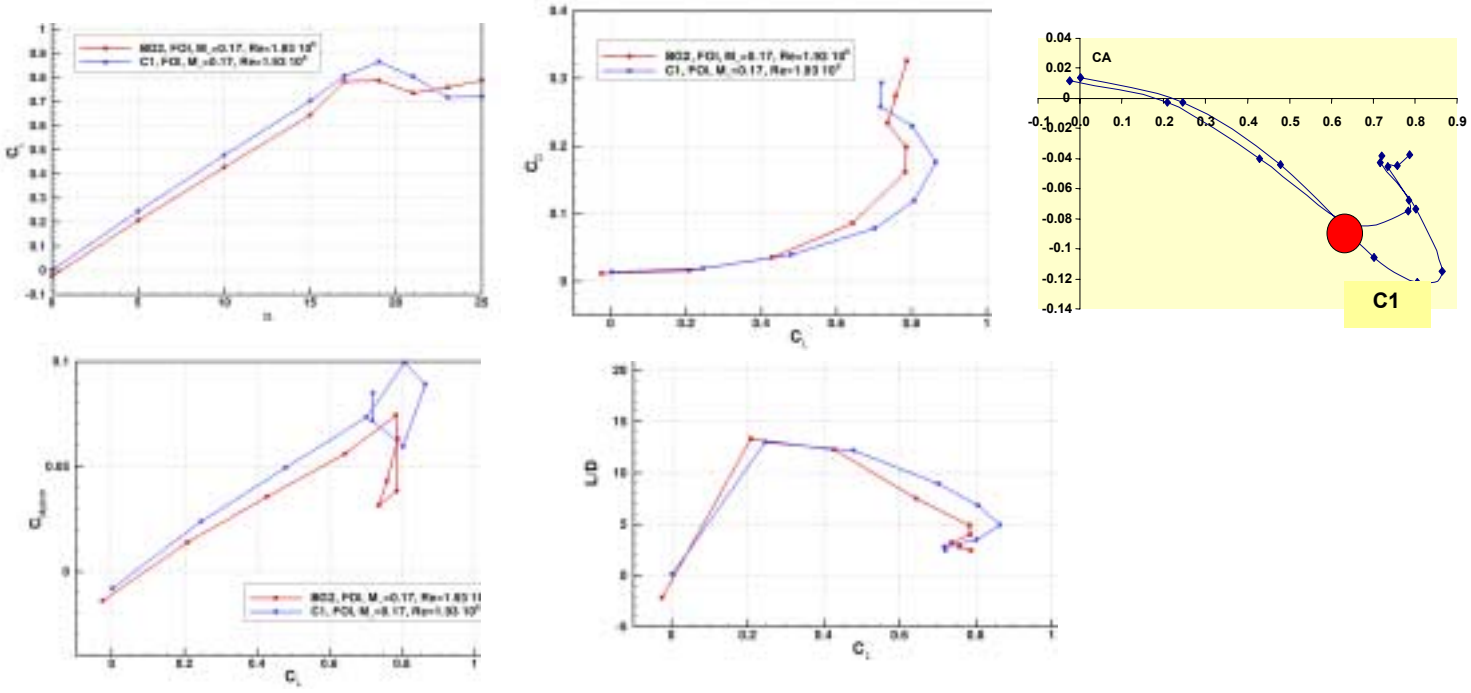

FIG. 21 BG2 & C1, Mach 0.17, Re = 1.93×10^6 (EDGE)

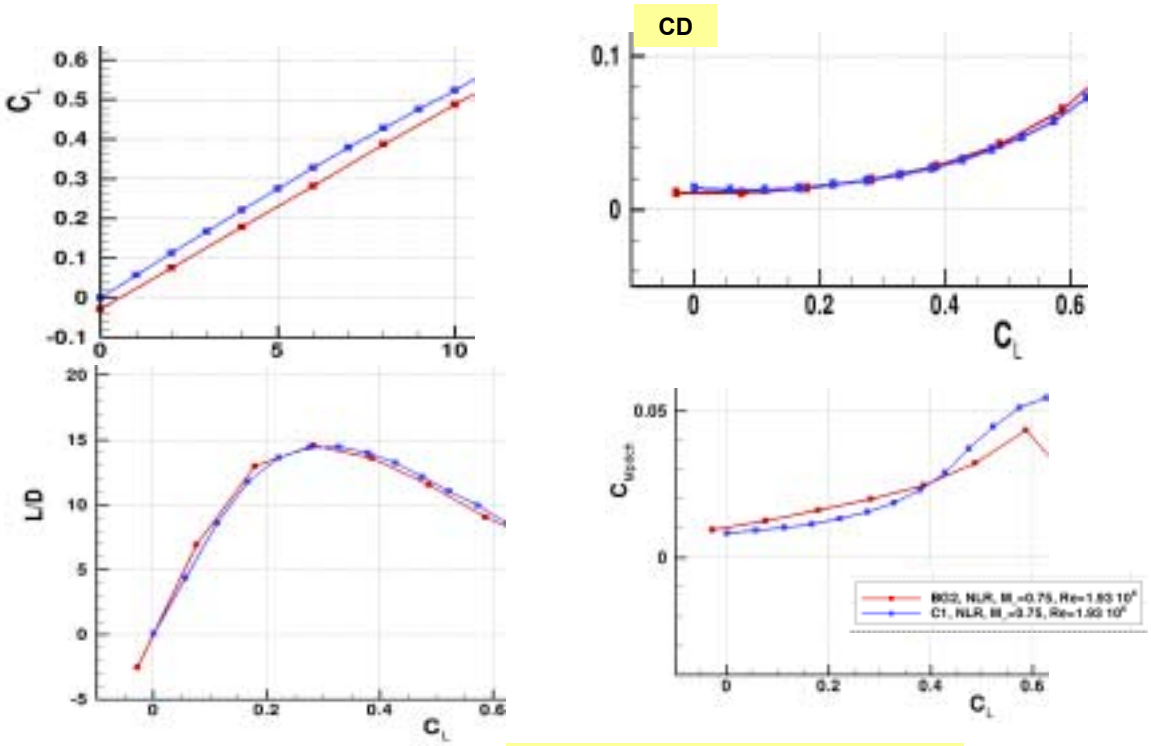

FIG. 22 BG2 & C1, Mach 0.75, Re = 1.93×10^6 (ENSOLV)

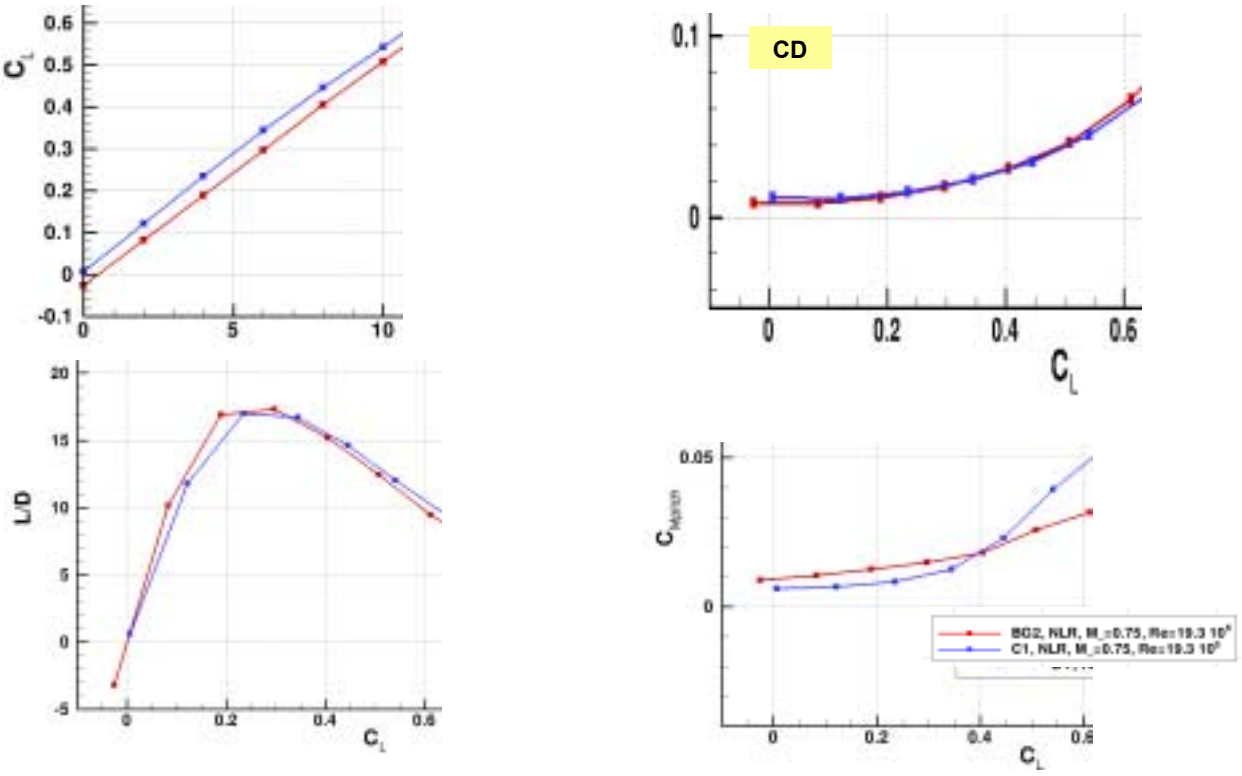

FIG. 23 BG2 & C1, Mach 0.75, Re = 19.3x10^6 (ENSOLV)

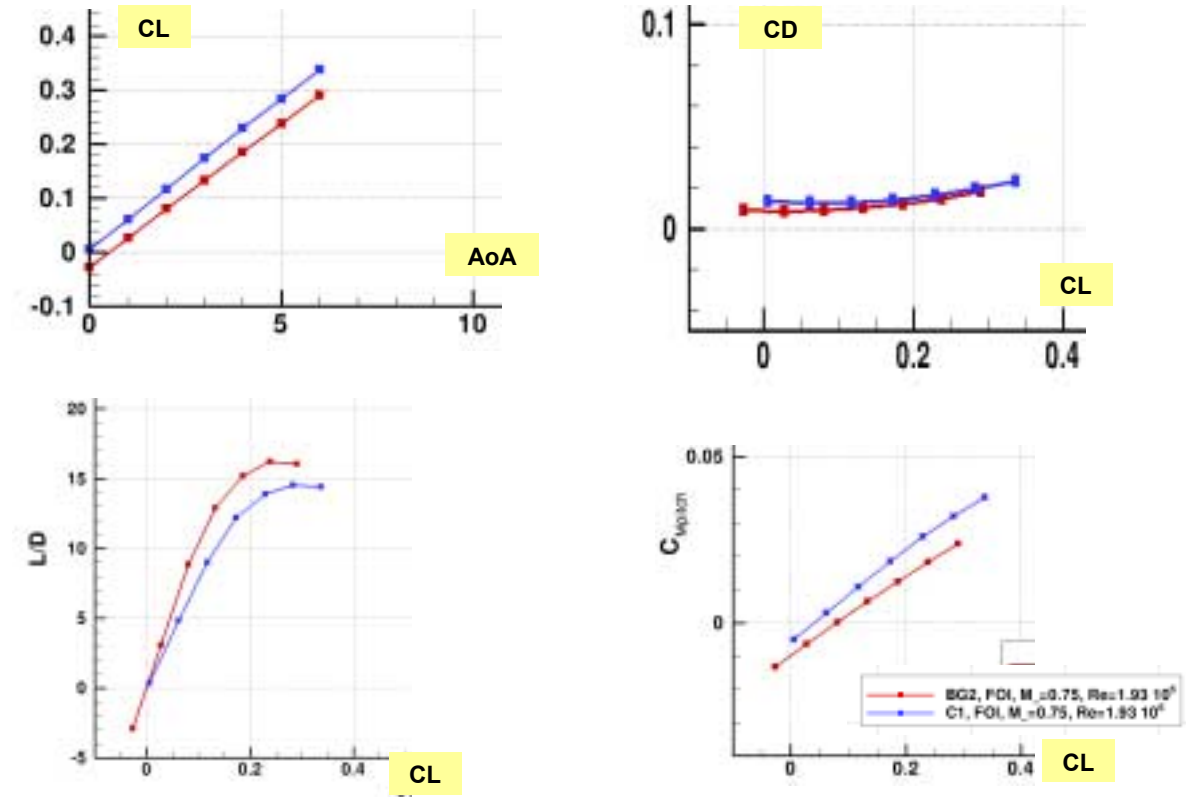

FIG. 24 BG2 & C1, Mach 0.75, Re = 1.93x10^6, (EDGE)

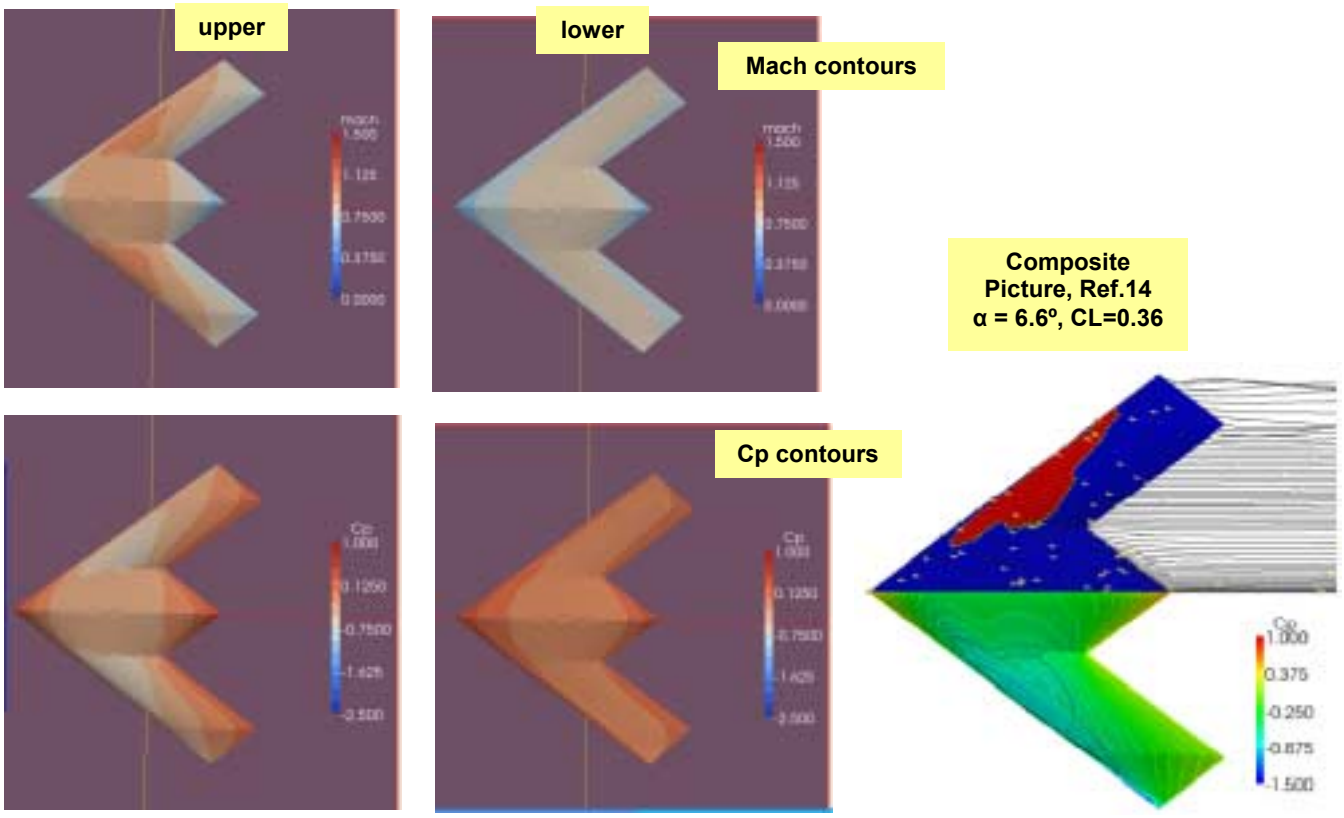

FIG. 25 BG2, Mach 0.75, α = 5º. Mach & Cp contours on upper & lower surfaces, Euler, CL= 0.268

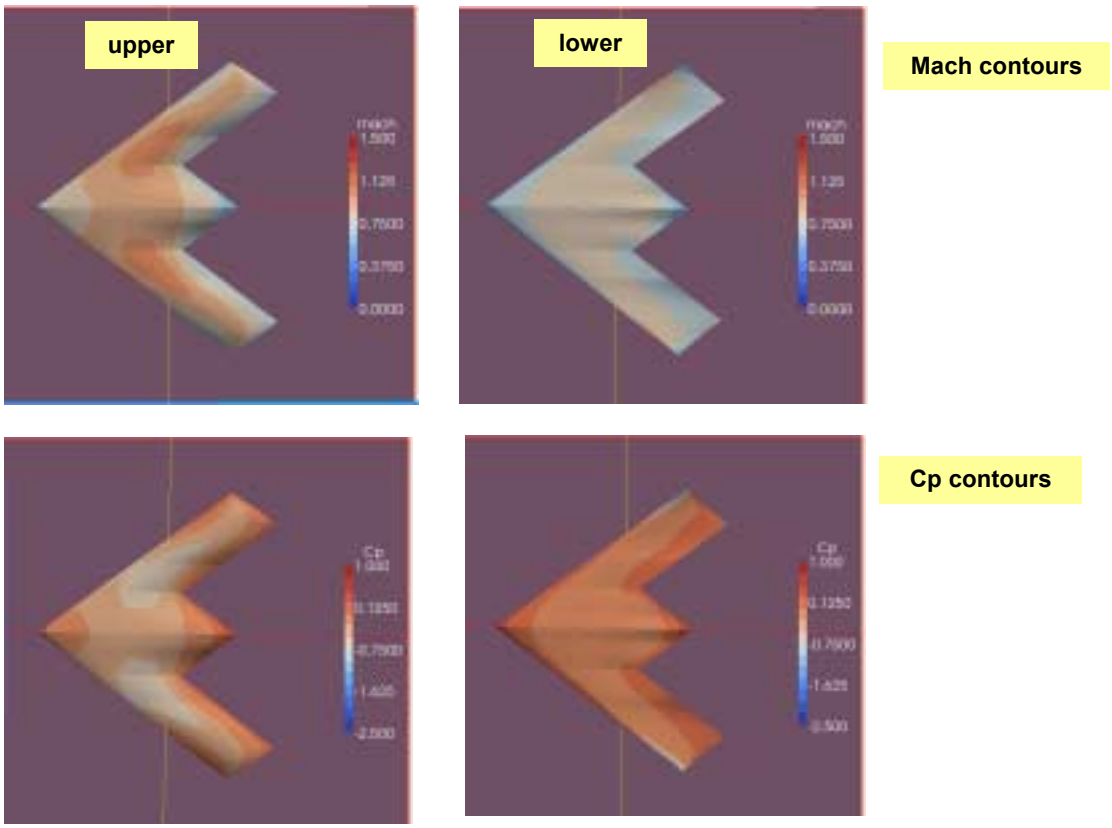

FIG. 26 C1, Mach 0.75, α = 5º. Mach & Cp contours on upper & lower surfaces, Euler, CL= 0.292